JPE 9-1-14

Sliding Mode Observer for Sensorless Control of IPMSM Drives

Young-Seok Jung† and Marn-Go Kim*

† Division of Mechanical Eng., Pukyong National University, Busan, Korea
* Division of Electrical and Control Eng., Pukyong National University, Busan, Korea

ABSTRACT

This paper presents a sliding mode observer for the sensorless control of interior permanent magnet synchronous motor (IPMSM) drives. The sliding mode observer has been presented as a robust estimation method. Most of these previous works, however, were not for an interior PMSM (IPMSM), but for a non-salient pole PMSM and its observer design is conducted in the stationary reference frame. Thus, in this paper, we investigate the design of a sliding mode observer and its driving characteristics for an IPMSM. The proposed sliding mode observer is designed in the rotating reference frame, and good drive performance is achieved even when the observer parameters are mismatched with those of an actual motor. The proposed method is applied to a 600W IPMSM, and, then, the measurement results are presented.

Keywords: Interior Permanent Magnet Synchronous Motor (IPMSM), Sliding mode observer, Sensorless control

1. Introduction

The permanent magnet synchronous motor (PMSM) has been widely used in many industrial applications because of its high efficiency, maintenance-free operation and high controllability. In order to obtain high performance of a PMSM, the information for rotor position is necessary. The rotor position can be obtained from some type of shaft sensor such as an optical encoder or resolver connected in the rotor shaft. However, these sensors introduce undesirable features such as increasing the driving cost and machine size. Therefore, a mechanical sensorless drive is desired for the PMSM, and, thus, various sensorless control algorithms have been investigated and reported in many publications[1-9].

Most sensorless control in a PMSM can be classified roughly into two categories: 1) back-emf estimation method[2,3,5-8] and 2) high frequency signal injection method[1]. The back-emf estimation method utilizes the dynamic model of a machine and estimates a rotor position from the calculated back emf. Because established back-emf is negligible at low speeds, this method is suited for middle or high speed operation. On the other hand, the high frequency signal injection method utilizes injected voltage or current signal for a salient pole PMSM. Among these two categories, the sliding mode observer based rotor position estimation can be classified as the back-emf estimation method.

It is shown in the literature that, for sensorless operation, the speed and/or position estimations are sensitive to parameter variations and the design of observer gain is tedious work. To improve the robustness of the controllers, a sliding mode controller has been proposed for some time.

Manuscript received Sep. 25, 2008; revised Nov. 19, 2008
† Corresponding Author: yousjung@pknu.ac.kr
Tel: +82-51-629-6165, Fax: +82-51-629-6150, PKNU
* Pukyong National University, Korea

While in the sliding mode, these controllers are insensitive to parameter variations and disturbances. Therefore, the sliding mode observer has been presented as a robust estimation method[5-8]. However, most of these previous work dealing with a sliding mode observer was not for an interior PMSM (IPMSM), but for a non-salient pole PMSM and its observer design is conducted in the stationary reference frame. For the IPMSM, the variation of inductance according to the rotor position makes it difficult to apply the conventional method directly.

Thus, we present the sliding mode observer for sensorless control of an IPMSM, and investigate the driving characteristics. At first, a mathematical model of an IPMSM based on the extended EMF in the rotating reference frame is considered, and then control loop design and investigation of the driving performance are carried out. Good drive performance is achieved from the proposed method.

This paper is organized as follows. The mathematical model of an IPMSM is reviewed in Section 2. A sensorless drive utilizing a sliding mode observer is presented in Section 3. To show the feasibility of the presented method, the simulations and experiments are carried out and illustrated in Section 4. Some conclusions are given in Section 5.

2. Mathematical Model of an IPMSM

The mathematical model of an IPMSM expressed in the extended EMF form is briefly described in this section[2-3]. The voltage equation of the IPMSM in the rotating d-q reference frame is given by (1).

$$\begin{bmatrix} v_d \\ v_q \end{bmatrix} = \begin{bmatrix} R_a + pL_d & -\omega L_q \\ \omega L_d & R_a + pL_q \end{bmatrix} \begin{bmatrix} i_d \\ i_q \end{bmatrix} + \begin{bmatrix} 0 \\ \omega K_E \end{bmatrix} \tag{1}$$

where v_d, v_q are the *d-q* axes applied voltages, i_d, i_q are the *d-q* axes currents, ω is the rotor speed, R is the armature winding resistance, L_d, L_q are the *d-q* axes inductances, K_E is the EMF constant, and p is a short notation of d/dt. By arranging the winding inductance in (1), the voltage equation could be rewritten as (2) and (3).

$$\begin{bmatrix} v_d \\ v_q \end{bmatrix} = \begin{bmatrix} R_a + pL_d & -\omega L_q \\ \omega L_q & R_a + pL_d \end{bmatrix} \begin{bmatrix} i_d \\ i_q \end{bmatrix} + \begin{bmatrix} 0 \\ E_{ex} \end{bmatrix} \tag{2}$$

$$E_{ex} = \omega[(L_d - L_q)i_d + K_E] - (L_d - L_q)(pi_q) \tag{3}$$

Because the exact position of the rotor is not known, it is necessary to use another reference frame, noted as the γ–δ frame, which lags by θ_e from the *d-q* reference frame. Transforming the equation (2) into the γ–δ frame, the following model in the rotating reference frame is obtained.

$$\begin{bmatrix} v_\gamma \\ v_\delta \end{bmatrix} = \begin{bmatrix} R_a + pL_d & -\omega L_q \\ \omega L_q & R_a + pL_d \end{bmatrix} \begin{bmatrix} i_\gamma \\ i_\delta \end{bmatrix} + \begin{bmatrix} e_\gamma \\ e_\delta \end{bmatrix} \tag{4}$$

$$\begin{bmatrix} e_\gamma \\ e_\delta \end{bmatrix} = E_{ex} \begin{bmatrix} -\sin\theta_e \\ \cos\theta_e \end{bmatrix} - (\hat{\omega} - \omega) L_d \begin{bmatrix} i_\delta \\ -i_\gamma \end{bmatrix} \tag{5}$$

where $\theta_e = \theta - \hat{\theta}$, $\hat{\theta}$ and $\hat{\omega}$ are the estimated position and estimated speed, respectively. It is noted from the equation (4) that the inductance is constant in the γ–δ frame, and this makes the design of the controller easier.

3. A Sliding Mode Observer Based Sensorless Driver

In order to design the sliding mode observer for the IPMSM, the voltage equation in (4) is rearranged as (6).

$$L_d \begin{bmatrix} pi_\gamma \\ pi_\delta \end{bmatrix} = -R_a \begin{bmatrix} i_\gamma \\ i_\delta \end{bmatrix} - \begin{bmatrix} e_\gamma \\ e_\delta \end{bmatrix} + \omega L_q \begin{bmatrix} i_\delta \\ -i_\gamma \end{bmatrix} + \begin{bmatrix} v_\gamma \\ v_\delta \end{bmatrix} \tag{6}$$

From (6), we can give the state equations representing the estimated current dynamics as (7).

$$L_d \begin{bmatrix} p\hat{i}_\gamma \\ p\hat{i}_\delta \end{bmatrix} = -R_a \begin{bmatrix} \hat{i}_\gamma \\ \hat{i}_\delta \end{bmatrix} - k \begin{bmatrix} sign(\hat{i}_\gamma - i_\gamma) \\ sign(\hat{i}_\delta - i_\delta) \end{bmatrix} + \hat{\omega} L_q \begin{bmatrix} i_\delta \\ -i_\gamma \end{bmatrix} + \begin{bmatrix} v_\gamma \\ v_\delta \end{bmatrix} \tag{7}$$

where $\hat{i}_\gamma$ and $\hat{i}_\delta$ denote the estimated currents and k is a constant observer gain. Subtracting (6) from equation (7) yields the dynamics of the error in the estimated currents:

$$L_d \begin{bmatrix} p\bar{i}_\gamma \\ p\bar{i}_\delta \end{bmatrix} = -R_a \begin{bmatrix} \bar{i}_\gamma \\ \bar{i}_\delta \end{bmatrix} + \begin{bmatrix} e_\gamma \\ e_\delta \end{bmatrix} - k \begin{bmatrix} sign(\bar{i}_\gamma) \\ sign(\bar{i}_\delta) \end{bmatrix} + (\hat{\omega} - \omega) L_q \begin{bmatrix} i_\delta \\ -i_\gamma \end{bmatrix} \tag{8}$$

where $\bar{i}_\gamma$ and $\bar{i}_\delta$ denote the observation errors. From the reaching condition, we can determine the condition for the

observer gain *k*. They are:

$$\bar{i}_\gamma(p\bar{i}_\gamma)<0 \quad \text{and} \quad \bar{i}_\delta(p\bar{i}_\delta)<0 \tag{9}$$

The inequities above can be satisfied when

$$k>\max\left(\left|e_\gamma\right|+\left|(\hat{\omega}-\omega)L_q i_\delta\right|,\left|e_\delta\right|+\left|(\hat{\omega}-\omega)L_q i_\gamma\right|\right) \tag{10}$$

It is noted from the equation (10) that the observer gain *k* when applied to the IPMSM should be larger than the induced back emf added with an additional term which is proportional to the error in the speed estimation.

The system behavior can be examined by applying the equivalent control method. The following are the conditions:

$$\bar{i}_\gamma = p\bar{i}_\gamma = 0,\ \bar{i}_\delta = p\bar{i}_\delta = 0 \tag{11}$$

From (5) and (8), the characteristics of a sliding mode observer on the sliding hyper-plane might be defined as:

$$Z \equiv k\begin{bmatrix} sign(\bar{i}_\gamma) \\ sign(\bar{i}_\delta)\end{bmatrix} = E_{ex}\begin{bmatrix} -\sin\theta_e \\ \cos\theta_e\end{bmatrix} + (\hat{\omega}-\omega)(L_q-L_d)\begin{bmatrix} i_\delta \\ -i_\gamma\end{bmatrix} \tag{12}$$

where the switching signal *Z* contains the information of the rotor position. Assuming that the error between the estimated speed and the actual speed is sufficiently small and applying low pass filtering for the switching signal *Z*, the filtered switching signal can be obtained as follows:

$$\tilde{Z} = \begin{bmatrix}\tilde{z}_\gamma \\ \tilde{z}_\delta\end{bmatrix} = E_{ex}\begin{bmatrix} -\sin\theta_e \\ \cos\theta_e\end{bmatrix} \tag{13}$$

From (13), the rotor position error can be derived as

$$\theta_e = -\tan^{-1}\left(\frac{\tilde{z}_\gamma}{\tilde{z}_\delta}\right) \tag{14}$$

When the proportional and integral (PI) compensator is used in the position estimation loop, the transfer function relating the estimated and actual rotor positions is given as follows[1]:

$$\frac{\hat{\theta}(s)}{\theta(s)} = \frac{K_p s + K_i}{s^2 + K_p s + K_i} \tag{15}$$

Fig. 2 shows the equivalent block diagram for position estimation. In this figure, the output of sliding mode observer θ_e can be obtained from a virtual feedback. This structure gives the equation (15). The PI controller gains are chosen from the estimating performance when its natural frequency ω_n and the damping ratio ζ_n is given:

$$K_p = 2\zeta_n\omega_n, \quad K_i = \omega_n^2 \tag{16}$$

The block diagram of the sliding mode observer based rotor position estimation derived above is shown in Fig. 1(a). And to compare with the conventional one, the block diagram of the sliding mode observer in the stationary reference frame is also shown in Fig. 1(b). The block diagram shown Fig. 1(a) can be used both for an IPMSM and a SPMSM, whereas the conventional one shown in Fig. 1(b) is just for a SPMSM.

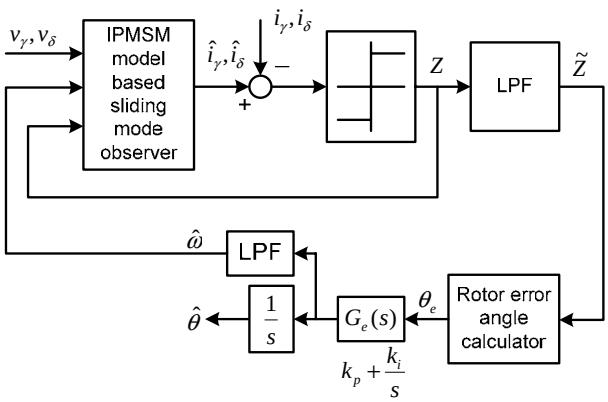

(a) Sliding mode observer in the rotating reference frame

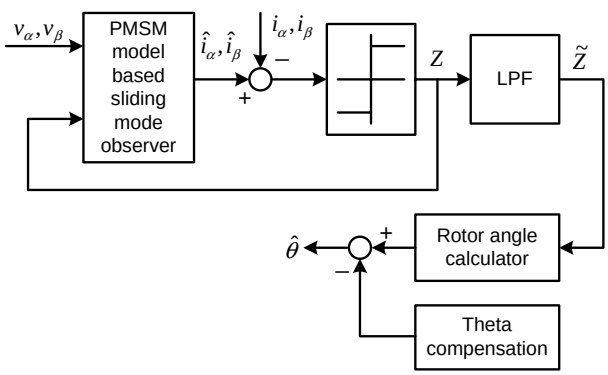

(b) Conventional sliding mode observer in the stationary reference frame only useful for the SPMSM drives

Fig. 1 Block diagrams of the sliding mode observer based rotor position estimation.

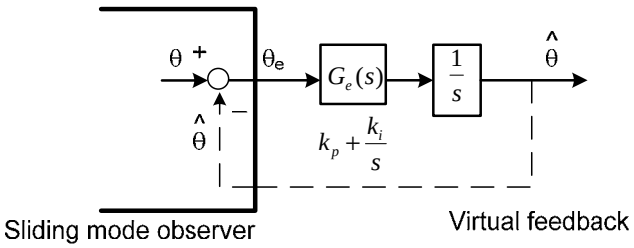

Fig. 2 Equivalent block diagram for the position estimation

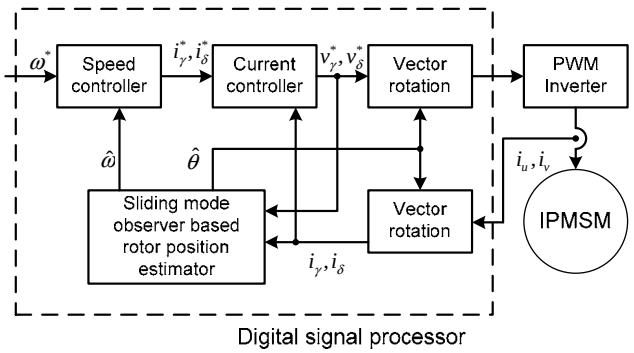

Fig. 3 Block diagram of the sliding mode observer based speed control system

Table 1 Parameters of tested IPMSM

Number of pole-pairs	3
Rated speed	3000 rpm
DC link voltage	120V
Armature resistance R_a	0.3 Ω
d-axes inductance L_d	4.04 mH
q-axes inductance L_q	8.20 mH

4. Simulation and Experimental Results

In this section, the rotor position estimation results based on the sliding mode observer are presented and their characteristics with respect to the parameter variations are also illustrated. The specifications of the IPMSM utilized in this research are listed in Table 1. Fig. 3 shows the overall block diagram of the sliding mode observer based sensorless speed control system. The sampling period for the current control and the rotor position estimation is chosen to be 0.1ms and the switching frequency of the PWM inverter is 10 kHz.

4.1 Simulation results

The sliding mode observer based sensorless control

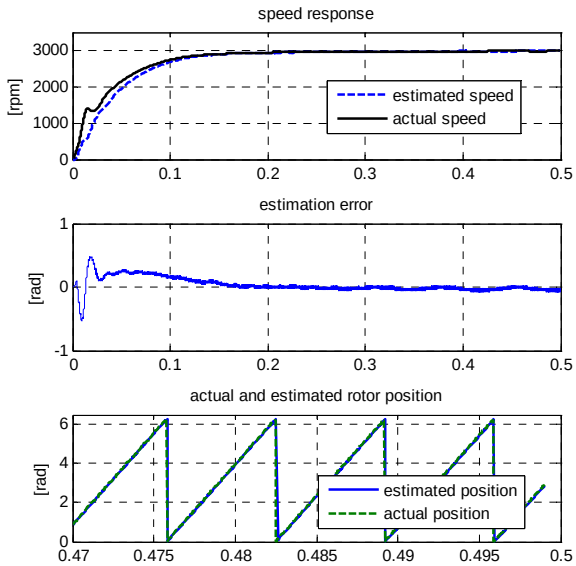

Fig. 4 Simulation results of speed response, estimation error, and actual and estimated rotor positions

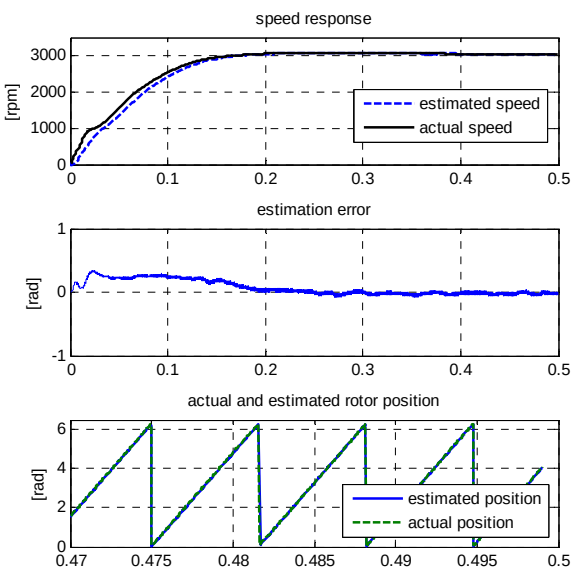

Fig. 5 Simulation results when R in the observer equals to 1/3 of resistor in motor

algorithm was simulated by Matlab/Simulink. The space vector PWM algorithm was applied and updated every 100 μs with respect to the switching frequency 10 kHz. Fig. 4 shows the simulation results when the motor was started from rest to 3000 rpm. For this purpose, the initial position of the actual rotor position is assumed to be known and used to initialize the initial position of the

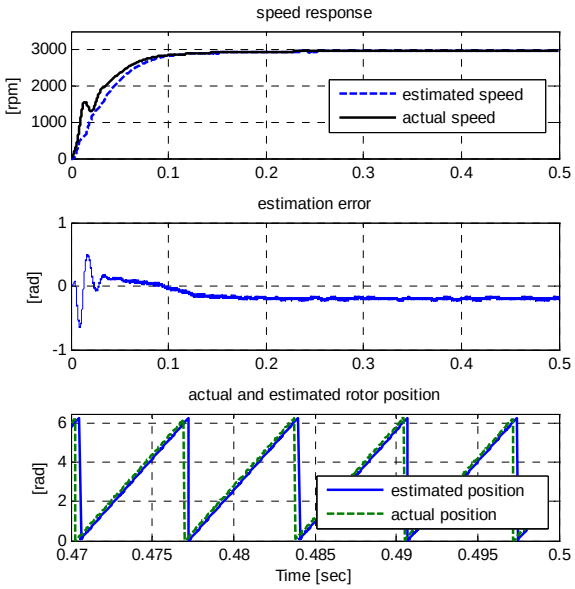

Fig. 6 Simulation results when L_q in the observer equals to 80% of L_q in motor

sliding mode observer. During the initial start-up period, there exists large position estimation error compared to steady state operation, which is to be expected from the analytical results as in (12), but its drive performance is not bad. The effect of the variation of a resistance in stator windings is considered in the simulation and the results are shown in Fig. 5. Even though there exists large difference between the actual motor and the observer parameters, the deviations in the start-up and the steady state operations are small compared to those for the exact parameter matching condition. However, for the case of inductance variation, this might be not the case. The variation of the inductance could give a position estimation error, and possibly even make the drive system unstable. Fig. 6 shows the simulation results when a q-axis inductance in the observer is equal to 80% of a nominal value, which shows stable operation, but the estimated position error is about 0.2 [rad] in the steady state. Careful consideration for this is required.

4.2 Experimental results

The control algorithms were implemented on a Texas Instruments TMS320F28016 low cost 32bit fixed-point

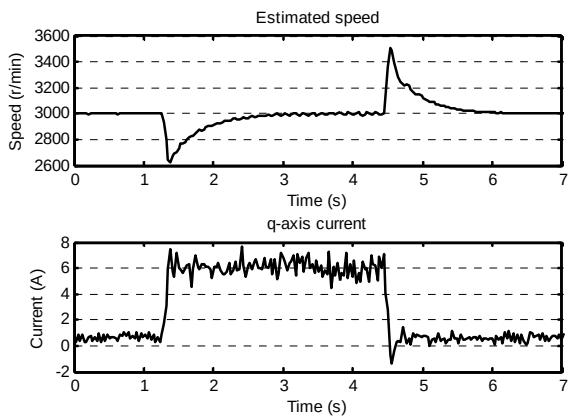

Fig. 8 Speed and q-axis current responses from real-time data logging for step changes of load torque (Speed reference: 3000 r/min, Load: 0 → 100% → 0)

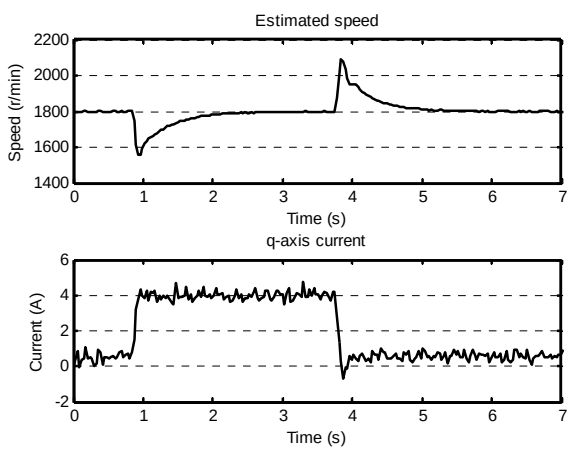

Fig. 7 Speed and q-axis current responses from real-time data logging for step changes of load torque(speed reference: 1800 r/min, Load: 0 → 70% → 0)

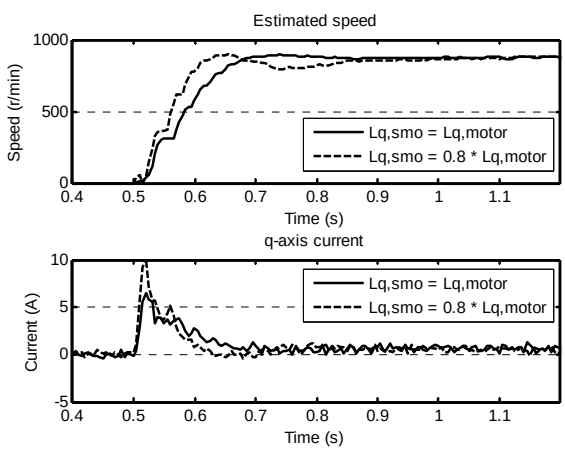

Fig. 9 Acceleration performances from rest to 900 [r/min] from real-time data logging when different q-axis inductances are used for the sliding mode observer

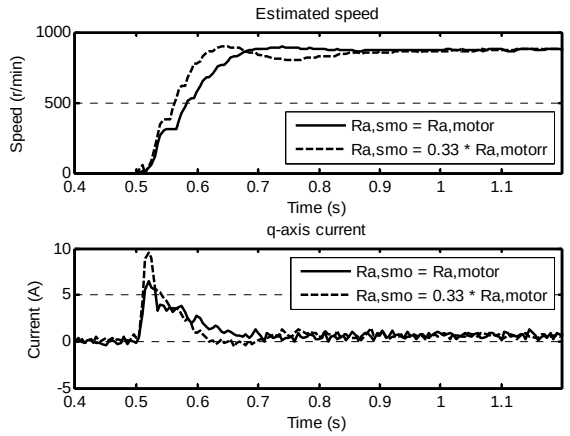

Fig. 10 Acceleration performances from rest to 900 [r/min] from real-time data logging when different armature resistances are used for the sliding mode observer

digital signal processor (DSP). In the experiment, we do not conduct the maximum torque per current operation. Instead, the q-axis current command is generated from the speed control loop and the d-axis current command is set to zero. And the used observer parameters are k = 300, K_p = 200, and K_i = 10000.

Figs. 7 and 8 show the response for a step change of 70% load torque at 1800 r/min and 100% load torque at 3000 r/min, respectively. As shown in these figures, good performance against load disturbance is obtained.

Figs. 9 and 10 show the acceleration performance from rest to 900 r/min when different observer parameters such as a q-axis inductance or an armature resistance are used. To start from zero speed, an initial rotor axis is aligned first with a predefined axis by applying a specific current vector, and this causes a 0.5sec delay in these figures. Even though a small perturbation can be observed, good drive performance against parameter variations is obtained.

When decreasing the rotor speed below 360 r/min under full load conditions, the speed fluctuation becomes large. In order to operate the drives below this speed, an additional method such as a high frequency signal injection should be considered.

5. Conclusions

This paper proposes a sliding mode observer for sensorless control of an interior permanent magnet synchronous motor. Different from the conventional sliding mode observer applied to a non-salient pole PMSM, in the proposed method, the sliding mode observer is designed in the rotating reference frame. The proposed method is applied to a 600W IPMSM, and then the simulation and experimental results are presented. When the speed reference or the load torque changes rapidly, position and speed estimation errors are caused. However, such errors are small, and their influence on the motor drives is minimal. Good drive performance is also observed when some parameter deviations of the sliding mode observer from those of the actual motor exist, such as q-axis inductance or armature resistance. But, because of possible unstable drive performance, a careful choice for the observer parameter is required, particularly for the inductance.

Appendix: Proof of the stability of the SMO

In order to satisfy the stability of the sliding mode observer, the equation (8) is required. From the equation (9), we have the following:

$$\begin{aligned} L_d\bar{i}_\gamma(p\bar{i}_\gamma) &= -R_a\bar{i}_\gamma^2 + e_\gamma\bar{i}_\gamma - ksign(\bar{i}_\gamma)\bar{i}_\gamma + (\hat{\omega}-\omega)L_q i_\delta\bar{i}_\gamma \\ &= \begin{cases} \bar{i}_\gamma\left[e_\gamma + (\hat{\omega}-\omega)L_q i_\delta - k\right] - R_a\bar{i}_\gamma^2, & \bar{i}_\gamma > 0 \\ \bar{i}_\gamma\left[e_\gamma + (\hat{\omega}-\omega)L_q i_\delta + k\right] - R_a\bar{i}_\gamma^2, & \bar{i}_\gamma < 0 \end{cases} \end{aligned} \quad \text{(A1)}$$

Similarly,

$$\begin{aligned} L_d\bar{i}_\delta(p\bar{i}_\delta) &= -R_a\bar{i}_\delta^2 + e_\delta\bar{i}_\delta - ksign(\bar{i}_\delta)\bar{i}_\delta - (\hat{\omega}-\omega)L_q i_\gamma\bar{i}_\delta \\ &= \begin{cases} \bar{i}_\delta\left[e_\delta - (\hat{\omega}-\omega)L_q i_\gamma - k\right] - R_a\bar{i}_\delta^2, & \bar{i}_\delta > 0 \\ \bar{i}_\delta\left[e_\delta - (\hat{\omega}-\omega)L_q i_\gamma + k\right] - R_a\bar{i}_\delta^2, & \bar{i}_\delta < 0 \end{cases} \end{aligned} \quad \text{(A2)}$$

Since $-R_a\bar{i}_\gamma^2 < 0$ and $-R_a\bar{i}_\delta^2 < 0$, the inequalities shown in the equation (8) can be satisfied when

$$k > \max\left(\left|e_\gamma\right| + \left|(\hat{\omega}-\omega)L_q i_\delta\right|, \left|e_\delta\right| + \left|(\hat{\omega}-\omega)L_q i_\gamma\right|\right) \quad \text{(A3)}$$

So the sliding mode observer is stable when equation (10) is satisfied.

References

[1] J. I. Ha, K. Ide, T. Sawa, and S. K. Sul, "Sensorless rotor position estimation of an interior permanent-magnet motor from initial states", *IEEE Trans. Ind. Appl*., Vol. 39, No. 3, pp. 761-767, May/Jun., 2003.

[2] S. Morimoto, M. Sanada, and Y. Takeda, "Mechanical sensorless drives of IPMSM with online parameter identification", *IEEE IAS*., Vol. 1, pp. 297-303, 2005.

[3] Z. Chen, M. Tomita, S. Doki, and S. Okuma, "An extended electromotive force model for sensorless control of interior permanent-magnet synchronous motors", *IEEE Trans. Ind. Electron*., Vol. 50, No. 2, pp. 288-295, Apr. 2003.

[4] N. Matsui, "Sensorless PM brushless DC motor drives", *IEEE Trans. Ind. Electron*., Vol. 43, No. 2, pp. 300-308, Apr. 1996.

[5] S. Chi, and L. Xu, "Position sensorless control of PMSM based on a novel sliding mode observer over wide speed range", *IEEE IPEMC*, pp. 597-605, 2006.

[6] K. L. Kang, J. M. Kim, K. B. Hwang, and K. H. Kim, "Sensorless control of PMSM in high speed range with iterative sliding mode observer", *in Conf. Rec. IEEE APEC*, Vol. 2, pp. 1111-1116, 2004.

[7] M. Elbuluk and C. Li, "Sliding mode observer for wide-speed sensorless control of PMSM drives", *in Conf. Rec. IEEE IAS.*, Vol. 1, pp. 480-485, 2003.

[8] Y. S. Han, J. S. Choi, and Y. S. Kim, "Sensorless PMSM drive with a sliding mode control based adaptive speed and stator resistance estimator", *IEEE Trans. Magnetics*, Vol. 36, pp. 3588-3591, Sep. 2000.

[9] K. Y. Cho, "Sensorless Control for a PM Synchronous Motor in a Single Piston Rotary Compressor", *Journal of Power Electronics*, Vol. 6, No. 1, pp. 29-37, Jan. 2006.

Young-Seok Jung received his B.S., M.S. and ph.D. degrees in Electrical Engineering from the Korea Advanced Institute of Science and Technology (KAIST), Daejon, Korea, in 1992, 1994, and 1999, respectively. He worked as a senior researcher for Hyundai Autonet, Powertrain Team, from 1999 to 2002. Since 2002, he has been with the Division of Mechanical Engineering at Pukyong National University, Korea, where he is now an associate professor. His research interests are in the area of power converter and variable speed motor drives. Dr. Jung is a member of the Korean Institute of Power Electronics (KIPE).

Marn-Go Kim received the B. S. degree in Electrical Engineering from Kyungpook National University in 1986, and the M. S. and Ph.D. degrees in Electrical Engineering from Korea Advanced Institute of Science and Technology in 1988 and 1991, respectively. From 1991 to 1994, he was with Korea Telecom Research Center, where he researched telecom power systems such as uninterruptible power supplies, DC/DC converters, and distributed power systems. Since 1995, he has been with the department of control and automation engineering, Pukyong National University, where he is now a professor. His research interests include modeling, analysis, and control of resonant converters, power semiconductor circuits, and soft switching converters. Dr. Kim is a member of KIPE and KIEE.